JOURNAL OF AIRCRAFT
Vol. 47, No. 1, January–February 2010

Engineering Notes

Lift Enhancement at Low Reynolds Numbers Using Self-Activated Movable Flaps

Jörg U. Schlüter*
Nanyang Technological University,
Singapore 639798, Republic of Singapore

DOI: 10.2514/1.46425

Nomenclature

C_d	=	drag coefficient
C_l	=	lift coefficient
c	=	chord length
L/D	=	lift-over-drag ratio
Re	=	Reynolds number ($U_\infty \cdot l/\nu$)
α	=	angle of attack

I. Introduction

IN RECENT years, interest in micro air vehicles (MAVs) is rising. The reason for that is the availability of micro- and nanotechnology necessary for the design of these vehicles, but also the emergence of new threats, especially in form of terrorism. MAVs promise to be able to be deployed in closed environments, such as buildings, subway tunnels, and dense forests, allowing reconnaissance, surveillance, and search and rescue missions, for which the use of humans is dangerous or even impossible.

To be able to operate in this environment, MAVs need to be small and capable to fly at low speeds, yet they need to be agile enough to move around corners and bends. Moreover, they have to be able to transport a payload, such as video surveillance equipment or sensors for chemical agent detection. So far, no operational MAV exists that fits within these operational limits.

The reason for this is that conventional aircraft designs have difficulties in providing sufficient lift and aerodynamic efficiency at low Reynolds numbers [1]. The low lift coefficients cause problems in the design of MAVs, because the often prohibitively large wings are required. Hence, novel methods to increase lift at low Reynolds numbers need to be considered.

A method to increase the lift coefficient, inspired by biological flows, is investigated here. Schatz et al. [2,3] reported that the use of a passive flap near the trailing edge results in a lift increase at high angles of attack. The use of a passive flap is inspired by the feather structure of a bird on the upper side of the bird's wing [4,5]. At high angles of attack, it can be observed that the feathers start to pop up (Fig. 1). Schatz et al. [2,3] investigated the use of a passive flap to emulate this behavior. Their force measurements at Reynolds numbers above $Re = 1,000,000$ showed an increase of lift of about 10%.

Kernstine et al. performed experiments on this passive flap configuration at Reynolds numbers around $Re = 330,000$ [6], with similar results. Kernstine et al. focused especially on the optimal placement of the flaps and determined that the flap should be located closer to the midchord rather than the trailing edge to obtain optimal results. The $C_{l,\max}$ increased by a maximum of 15%.

The role of the flap is to capture the trailing edge flow separation and to prevent it from creeping upstream. This allows the flow to be attached on a larger portion of the wing than would be the case without and, as such, sustain higher angles of attack without stalling. The advantage of this flap is that it is a very simple and robust device that does not require complex mechanisms, such as conventional slats and flaps. It is easy to install and even retrofit existing aircraft.

Here, the possibility of applying this method to low Reynolds numbers at about $Re = 30,000$–$40,000$, which is a more suitable range for MAV, is investigated. The aerodynamics of airfoils at this Reynolds number range are especially challenging due to the presence of laminar flow separation and the nonlinearities, such as hysteresis effects, associated with it. A water tunnel is used to visualize the flow and to measure the effect of the flap at this Reynolds number range.

II. Water Tunnel Setup

The water tunnel is a model (from Long Win Science and Technology Corporation) with a contraction ratio of 1:6 and a test section size of 0.3 m wide × 0.3 m high × 1.0 m long. The velocity range is from 0–0.65 m/s. The flow uniformity is high, with a maximum velocity change in the core test section of less than 2% and a turbulence intensity of less than 1%.

Forces are measured with a Chroma three-component force balance, measuring lift, drag, and moments. The balance was calibrated with static loads right before the measurements. The maximum load of the balance is 20 N in lift and drag direction. The uncertainties of the load cells are given by the manufacturer as 0.5% of the full load, which translates into a maximum absolute error of 0.1 N.

III. Water Tunnel and Balance Validation

First, measurements are performed to test the water tunnel setup and to compare the current measurements with experimental data available from the literature. The data are compared with measurements performed by Selig et al. [7,8], who performed measurements on airfoils at similar Reynolds numbers. The airfoil that is used is the SD8020 because, for this airfoil, the measurements of Selig et al. were especially detailed in this Reynolds number range. The airfoil model for the current measurements was manufactured out of aluminum, using computer-numerically controlled cutting and polished to reduce the roughness. The chord length is 70 mm. With a flow speed of 0.58 m/s, a Reynolds number of $Re = 40,600$ is obtained.

Figure 2 shows the measurements of the lift curve in comparison with the literature data. It can be seen that there is a good agreement of the lift data with the measurements of Selig et al. [7,8], especially in determining the onset of stall and the measurement of the maximum lift coefficient. However, the current measurements show a less-sudden loss of lift at high angles of attack. This can be associated with the surface roughness of the model as it increases the turbulence levels on the airfoil. The average surface roughness of the current model is measured as 1.839 μm. Selig et al. did not report the roughness, but they show that the application of a tripwire reduces

Presented as Paper 4195 at the 39th AIAA Fluid Dynamics Conference, San Antonio, TX, 22 June–25 May 2009; received 20 July 2009; revision received 7 October 2009; accepted for publication 7 October 2009.

*Assistant Professor, School of Mechanical and Aerospace Engineering, 50 Nanyang Avenue; schluter@ntu.edu.sg. Senior Member AIAA.

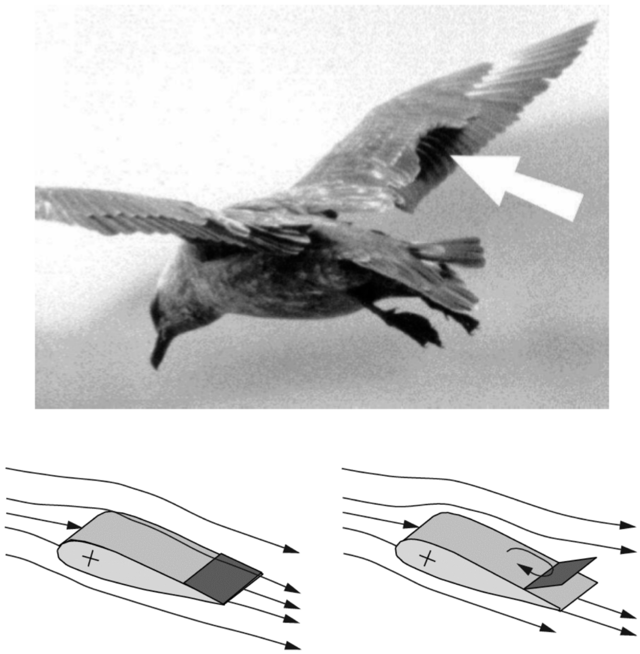

Fig. 1 Principle of a movable flap at high angles of attack: seagull at landing (top) and in-principle drawing (bottom). (Both pictures from Schatz et al. [2,3].)

nonlinear effects, as seen at very low angles of attack and high angles of attack.

A drag measurement on an airfoil at a low Reynolds number is particularly difficult, as the absolute forces measured are relatively small. This results in relatively high uncertainties of the measurements. Selig et al. [7,8] does not report drag measurements of the SD8020 airfoil at that Reynolds number, presumably due to the same issue, but has performed drag measurements at a Reynolds number of $Re = 60,000$. Figure 3 shows the current lift-over-drag measurements at Reynolds number $Re = 40,000$ compared with the data from Selig et al. at Reynolds number $Re = 60,000$. Although there is a good agreement between the two measurements, the uncertainty of the load cell measurements is relatively high, as can be seen on the error bars. Hence, the current measurements cannot claim that they are sufficiently certain to allow conclusions to be drawn. However,

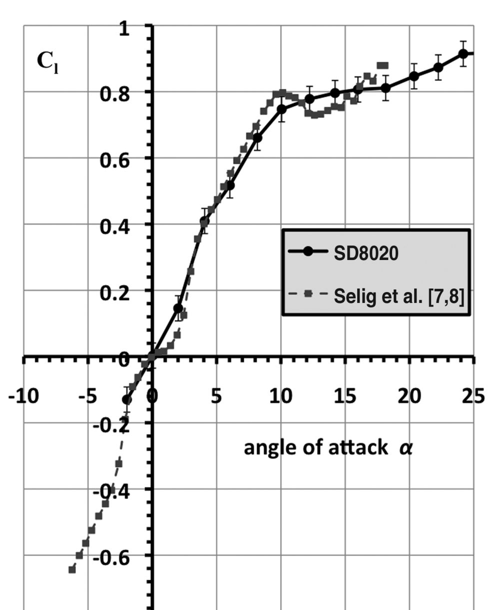

Fig. 2 Lift curve of the SD8020 at $Re = 40,600$. Comparison of lift measurements with literature data.

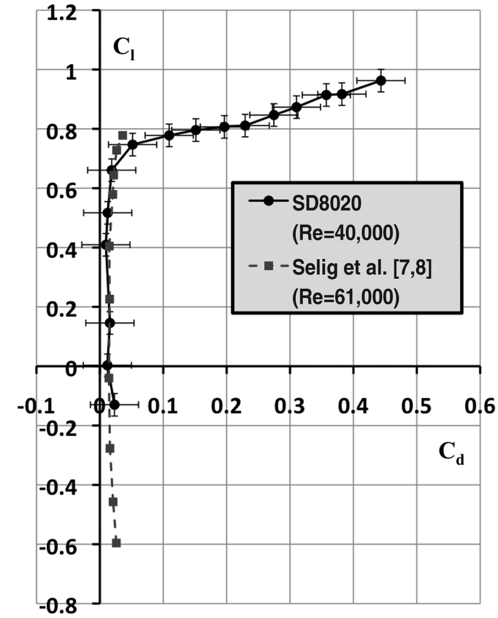

Fig. 3 Lift-over-drag measurement of the SD8020 airfoil compared with literature data.

the similarities of the current measurements with the data from Selig et al. give confidence that the water tunnel setup and the balance provide a good experiment to examine the lift characteristics of an airfoil at a low Reynolds number.

IV. Force Measurements with a Movable Flap

Three different airfoils are examined here: the NACA0012, the SD8020, and the NACA4412. On the latter two, parameter studies on the optimal placement of the flap have been performed.

Carbon fiber material with a total weight of about 5 g is used for the fabrication of the flap. The airfoils have a chord length of 60 mm for the NACA0012 and 70 mm for the SD8020 and NACA4412. The airfoils are 300 mm immersed in the water in the spanwise direction, leaving a gap of less than 10 mm between the tunnel floor and the tip of the wing.

Because the thickness of the flap will modify the airfoil shape slightly, control measurements of the smooth airfoils with the flap attached, but fixed to prevent deployment, are performed. For the symmetric airfoils NACA0012 and SD8020, the flaps are attached on both sides of the airfoil to assure the symmetry of the airfoils. No significant difference in the lift measurements between the smooth airfoil and the airfoil with the flaps attached have been found. Furthermore, the sweep direction does not play a role.

A. NACA0012 Airfoil

The NACA0012 is a relatively slender airfoil and is more prone to leading edge stall, especially at low Reynolds numbers. The airfoil chord length is 60 mm. The flap length is 10 mm and is mounted flush with the trailing edge of the airfoil, as Schatz et al. [2,3] reported this as the location of the flap in their measurements. With a flow speed of 0.51 m/s, this translates to a Reynolds number of $Re = 30,600$.

Figure 4 shows the measured lift curves with and without the flaps. It can be seen that the lift curves are almost identical at low angles of attack. At high angles of attack, stall occurs rapidly for the smooth airfoil without a flap (solid line with circular symbols). The lift curve with the flap has smoother stall characteristics and provides more lift at angles of attack past stall (dashed line with square symbols). For example, for an angle of attack of 15 deg, the airfoil with the flap creates about 15% more lift than without.

In Fig. 4, measurements of Selig et al. [7,8] on a NACA0009 at $Re = 40,000$ are shown (triangular symbols). The data show a similar behavior compared with the NACA0012 airfoil but show

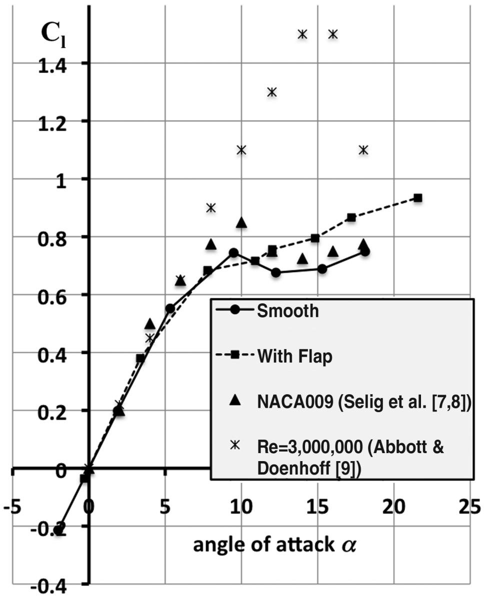

Fig. 4 Lift curve of the NACA0012.

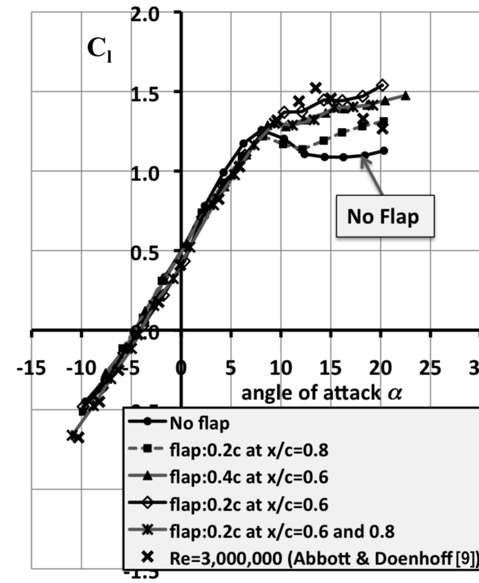

Fig. 6 Lift curve of the NACA4412 at $Re = 40,600$.

higher lift coefficients. The higher lift coefficients can be associated to the higher Reynolds number these measurements were taken.

Figure 4 also compares the measurements of Abbott and Doenhoff [9] of the NACA0012 at $Re = 3,000,000$ to the current measurements (star-shaped symbols). The lift slope at low angles of attack is identical to the current measurements. However, at high Reynolds numbers, the airfoil stalls at higher angles of attack. This results in a $C_{l,\max}$ that is almost twice as high as that at low Reynolds numbers. This underlines the challenges of MAVs to produce sufficient lift at low Reynolds numbers.

B. SD8020 Airfoil

Because Kernstine et al. [6] reported that a better position of the flap would be farther upstream of the trailing edge, a parameter study on the size and location of the flaps is performed. The configurations that have been investigated are the following:

1) Case 1 configurations have no flaps.

2) Case 2 configurations have airfoils with flaps of $0.2c$ length at $x/c = 0.8$ (flush with the trailing edge).

3) Case 3 configurations have airfoils with flaps of $0.4c$ length at $x/c = 0.6$ (large flap, flush with trailing edge).

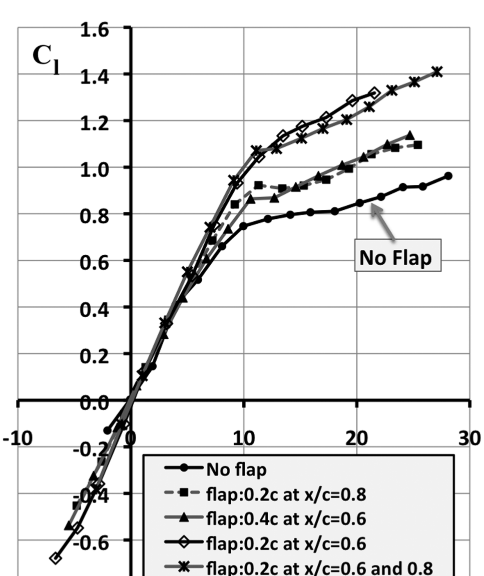

Fig. 5 SD8020 at $Re = 40,600$ with different flap configurations.

4) Case 4 configurations have airfoils with flaps of $0.2c$ length at $x/c = 0.6$.

5) Case 5 configurations have airfoils with two flaps each of $0.2c$ length at $x/c = 0.6$ and $x/c = 0.8$.

The chord length for this airfoil is 70 mm. With a flow speed of 0.58 m/s, a Reynolds number of $Re = 40,600$ is obtained.

Figure 5 shows the results for the different flap configurations. It can be seen that all of the flap configurations increase the lift substantially at high angles of attack when compared with the smooth airfoil. Case 2, in which the flap is close to the trailing edge, corresponds to the cases investigated by Schatz et al. [2,3] and the NACA0012 experiment of this study and shows an increase of about 15% at an angle of attack of 15 deg. An increase of the flap size (case 3) does not provide an advantage, in terms of lift, over the smaller flap.

Moving the flap upstream (case 4), however, creates quite substantially higher lift at high angles of attack. At an angle of attack of 15 deg, the lift has increased by almost 50%. Using an additional flap close to the trailing edge (case 5) does not provide a substantial advantage over the single flap.

C. NACA4412 Airfoil

The final airfoil under investigation is that of the NACA4412. The NACA4412 is a popular choice for a large number of conventional aircraft. As a relatively high-cambered thick airfoil, it provides high lift coefficients. The airfoil chord length of the model is 70 mm, the flow speed is0.58 m/s, and hence, the Reynolds number is 40,600. As flaps, the same configurations are used as with the SD8020 airfoil (cases 1–5).

The measurements show that using the flaps improves the stall behavior (Fig. 6). In case 2, with a flap at $0.8c$, the lift curve is almost identical to that without flaps. Stall occurs at an angle of attack of 8 deg, but when increasing the angle of attack, the flap deploys at an angle of attack of 11 deg and recovers some of the lift.

The other cases improve the lift as well; again, the flap with a length of $0.2c$ at $x/c = 0.6$ performs the best. In the latter case, the lift characteristics of the airfoil are almost as good as in the high Reynolds number range, also shown in Fig. 6.

V. Conclusions

Lift enhancement techniques using movable, passive flaps on the extrados of the airfoil are investigated at low Reynolds numbers, especially with a focus on the application to MAVs. The measurements show that the flaps can increase the lift dramatically near stall.

In the case of the SD8020 airfoil, which is popular for MAV designs, the improvement with a flap length of $0.2c$ at $x/c = 0.6$ achieved an increase of lift of almost 50%. All of the flap configurations tested demonstrated that the lift breakdown at increasing angles of attack is less severe, which leads to gentler flight characteristics.

This lift increase offers tremendous opportunities to miniaturize the MAV or to increase the payload. It is a simple and robust, yet effective, measure for MAV designs.

Acknowledgments

The support of the Defence Science Organization Singapore as part of the feasibility study for nano air vehicles is gratefully acknowledged. Special thanks are extended to undergraduate student Tan Jing Ru for assistance in performing some of the measurements.

References

[1] Mueller, T. J., "An Overview of Micro Air Vehicle Aerodynamics," *Fixed and Flapping Wing Aerodynamics for Micro Air Vehicle Applications*, edited by T. J. Mueller, Vol. 195, Progress in Astronautics and Aeronautics, AIAA, New York, 2001, pp. 1–10.

[2] Schatz, M., Knacke, T., Thiele, F., Hage, W., Bechert, D., and Meyer, R., "Separation Control by Self-Activated Movable Flaps," AIAA Paper 2004-1243, Jan. 2004.

[3] Schatz, M., Knacke, T., Thiele, F., Hage, W., Bechert, D., and Meyer, R., "Separation Control by Self-Activated Movable Flaps," *AIAA Journal*, Vol. 45, No. 1, 2007, pp. 191–199. doi:10.2514/1.23507

[4] Bechert, D. W., Bruse, M., Meyer, R., and Hage, W. B., "Biological Surfaces and Their Technological Application: Laboratory and Flight Experiments on Drag Reduction and Separation Control," AIAA Paper 1997-1960, June 1997.

[5] Bechert, D. W., Bruse, M., Meyer, R., and Hage, W. B., "Biological Surfaces and Their Technological Application," *Naturwissenschaften*, Vol. 87, No. 4, 2000, pp. 157–171. doi:10.1007/s001140050696

[6] Kernstine, K., Moore, C., Cutler, A., and Mittal, R., "Initial Characterization of Self-Activated Movable Flaps: 'Pop-Up Feathers'," AIAA Paper 2008-0369, Jan. 2008.

[7] Selig, M. S., Guglielmo, J. J., Broern, A. P., and Giguere, P., *Summary of Low Speed Airfoil Data*, Vol. 1, SoarTech Aero, Virginia Beach, VA, 1995.

[8] Selig, M. S., Guglielmo, J. J., Broern, A. P., and Giguere, P., "Experiments on Airfoils at Low Reynolds Numbers," AIAA Paper 1996-0062, Jan. 1996.

[9] Abbott, I. H. and Doenhoff, A. E., *Theory of Wing Sections*, Dover, New York, 1959.